Dual-Mode X-Band EPR Study of Two Isomers of the Endohedral Metallofullerene Er@C_{82}

Y. Sanakis,[†] N. Tagmatarchis,[‡,§] E. Aslanis,[‡] N. Ioannidis,[†] V. Petrouleas,[†] H. Shinohara,[§] and K. Prassides*[,†,‡]

Institute of Materials Science, NCSR "Demokritos" 153 10 Ag. Paraskevi, Athens, Greece
School of Chemistry Physics and Environmental Science University of Sussex, Brighton BN1 9QJ, UK
Department of Chemistry, Nagoya University Nagoya 464-8602, Japan

Received July 17, 2001
Revised Manuscript Received August 19, 2001

Endohedral metallofullerenes are novel forms of fullerene-based materials in which metal atoms are encapsulated within the fullerene cages. Their production, separation, and isolation in isomer-pure forms are now quite advanced, and a plethora of materials, based primarily on lanthanides and groups 3 and 2 elements, has been structurally and electronically characterized.[1] Information on the electronic structure of monometallofullerenes and the degree of interfullerene electron transfer has come from the analysis of the hfs of EPR-active systems such as M@C_{82} (M = La, Y, Sc).[2] In contrast, no well-resolved EPR hfs are observed for lanthanide metallofullerenes, Ln@C_{82} (Ln = Ce, ..., Lu).[3] This has precluded detailed study of their electronic properties thus far. Recently, we have studied a series of single-isomer Er^{3+} metallofullerenes, which form in comparatively high yields.[4] Here we report a dual-mode X-band EPR study of two isomers of Er@C_{82} at low temperature. The observed EPR spectra differ from those of M@C_{82} (M = La, Y, Sc) in that the observed signals are due mainly to the encaged Er^{3+} ion, which interacts only weakly with the C_{82}^{3-} cage. Both isomers are characterized by strongly anisotropic **g**-tensors, with small differences in the exchange-coupling strength accounting for the dramatically different spectra of the two isomers.

Figure 1 shows the X-band EPR spectra of the Er@C_{82}(I) isomer (C_{2v} symmetry)[5] below 2500 G at 4.2 K for perpendicular and parallel polarization of the microwave field with respect to the external magnetic field. In perpendicular mode, transitions are observed at $g \approx 20$, 12.6, 4.5, and 3, whereas in parallel mode at $g \approx 22$ and 18. A very weak radical signal was detected at low microwave power at $g = 2$, but this represented a negligible fraction of centers and was attributed to cages without incorporated Er^{3+} ions.[4]

Low-field transitions are expected from the Er^{3+} ion, but it is unlikely that the observed resonances arise solely from the Er^{3+} ion. The existence of resonances both in parallel and perpendicular polarization and the absence of signals attributable to a noninteracting $S = {}^1/_2$ radical from the C_{82} cage indicate an interaction between the two species. A full account of this interaction, in conjunction with the interaction of the individual spins with their environment, is very complicated and requires knowledge of the electron-density distribution, currently unavailable. However, a basic understanding of the system can be achieved by the following spin-Hamiltonian approach, which treats the two interacting species as localized spins and ignores interfullerene interactions.

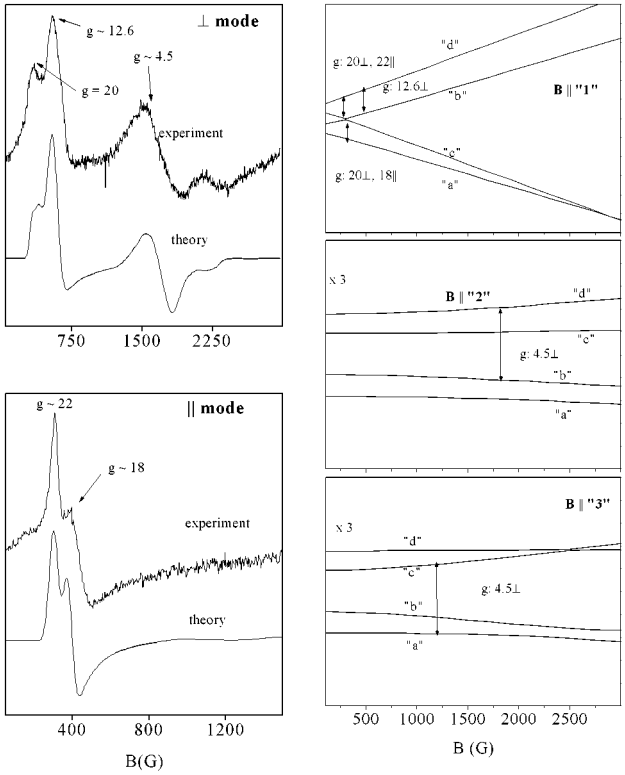

Figure 1. (Left panel) X-band EPR spectra of Er@C_{82}(I) for perpendicular (upper) and parallel (lower) polarization of the microwave field. The theoretical spectra were calculated as described in the text. *EPR* (Bruker ER 200D upgraded) *conditions:* $T = 4.2$ K, modulation amplitude, 10 Gpp, microwave power, 31 mW, microwave frequency, 9.60 GHz (perpendicular) and 9.33 GHz (parallel)**.** (Right panel) Dependence of the energy levels on **B** for **B** along the three principal axes (1, 2, 3) of the $\mathbf{g}_E$ tensor. Arrows indicate the transitions that contribute to the various signals. The labeling (a−d) of the levels corresponds to the ordering in energy at zero field.

The Er^{3+} ion ($4f^{11}$) is characterized by a $J = {}^{15}/_2$ ground-state manifold.[6] In a crystal field of low symmetry, this manifold splits into eight doublets. The crystal field splitting of the doublets can be large in Er^{3+} complexes, and this is the case in Er_2@C_{82}.[7] Here it is assumed to be much larger than the Zeeman term (at X band), the spin−spin interaction with the spin of the C_{82} cage, and the thermal energy at liquid He temperatures. Accordingly, the low-temperature properties are determined only by the ground doublet, which can be treated with an effective spin, $S_E = {}^1/_2$. The three-principal components g_1, g_2, and g_3 of the $\mathbf{g}_E$ tensor of this doublet, may be very different extending from large (>10) to small (<2) values (see below). On the other hand, the carbon cage is assumed to behave as an isotropic radical ($S_c = {}^1/_2$) with $g_c \approx 2.0$. A weak exchange interaction, treated as a tensor **J,** is assumed to couple the two spins. The following spin Hamiltonian,

[†] NCSR "Demokritos".
[‡] University of Sussex.
[§] Nagoya University.

(1) Shinohara, H. *Rep. Prog. Phys.* **2000**, *63*, 843−892.
(2) Johnson, R. D.; de Vries, M. S.; Salem, J. R.; Bethune, D. S.; Yannoni, C. S. *Nature* **1992**, *355*, 239−240; Kato, T.; Bandou, S.; Inakuma, M.; Shinohara, H. *J. Phys. Chem.* **1995**, *99*, 856−858.
(3) Knapp, C.; Weiden, N.; Dinse, K. P. *Appl. Phys. A* **1998**, *66*, 249−255.
(4) Tagmatarchis, N.; Aslanis, E.; Shinohara, H.; Prassides, K. *J. Phys. Chem. B* **2000**, *104*, 11010−11012; Tagmatarchis, N.; Aslanis, E.; Prassides, K.; Shinohara, H. *Chem. Mater.* **2001**, *13*, 2374−2379.
(5) The Er@C_{82}(I, II) isomers were produced by the composite rod arc-discharge burning method and were separated and isolated in isomer-pure form by a three-stage HPLC procedure, as described before.[4]
(6) Abragam, A.; Bleaney, B. In *Electron Paramagnetic Resonance of Transition Ions*; Dover Publications: New York, 1986.
(7) McFarlane, R. M.; Wittmann, G.; van Loosdrecht, P. H. M.; de Vries M.; Bethune, D. S.; Stevenson, S.; Dorn, H. C. *Phys. Rev. Let.* **1997**, *79*, 1397−1400.

10.1021/ja016636n CCC: $20.00
Published on Web 09/15/2001

including the Zeeman term, was then used:[8]

$$\mathbf{H} = \mathbf{S_E}\cdot\mathbf{J}\cdot\mathbf{S_c} + \beta\mathbf{B}\cdot\mathbf{g_E}\cdot\mathbf{S_E} + \beta\mathbf{g_c}\mathbf{B}\cdot\mathbf{S_c} \qquad (1)$$

Diagonalization of eq 1 results, in general, into the formation of four ground-state levels among which a number of EPR transitions are possible. An initial search for parameter combinations that would reproduce important features of the spectra indicated that: (a) the exchange coupling, **J**, is weak and anisotropic with one of its components close to zero, (b) the $\mathbf{g_E}$ tensor is characterized by one large component on the order of 18−20 and two small ones close to zero, and (c) assuming parallel orientation of the **J** and $\mathbf{g_E}$ tensors, the largest component of **J** is associated with the largest component of $\mathbf{g_E}$.

With the above restrictions the simulations converged to the theoretical spectra[9] of Figure 1. The parameters used to obtain these are: $g_1 = 19.0$, $g_2 = 0.0$, $g_3 = 0.6$, and $\mathbf{J} = (0.54, 0.18, 0.01)$ cm^{-1}. A small distribution in the J_i values of 0.004 cm^{-1} was assumed in the simulations. This corresponds to 1.6% of the isotropic value, $J_{iso} = (J_1 + J_2 + J_3)/3 = 0.243$ cm^{-1} and affects significantly the line shape. The corresponding energy level diagram is shown as a function of the magnetic field along the three principal orientations in the right panel of Figure 1. The various EPR transitions are also indicated. Clearly, the exchange coupling mixes considerably the levels at low fields for **B**||"1" and creates EPR transitions permissible in parallel mode. At high fields or perpendicular orientations (**B**||"2" or "3"), the transitions pertain their $\Delta m_s = \pm 1$ character.

The reproduction of the spectral features in Figure 1 is very satisfactory and supports the approach taken. It is possible that the details of the simulation could be further improved by relaxing the constraint of the parallel orientation of the $\mathbf{g_E}$ and **J** tensors, but this would complicate considerably the analysis and not add much to our understanding of the system.

Figure 2 shows the EPR spectra of Er@C_{82}(II) isomer. For this isomer, EPR signals are observed at very low fields (<550 G) both in parallel and perpendicular polarization, differing dramatically from the spectra obtained for Er@C_{82}(I). They are reminiscent of those obtained for non-Kramers systems.[10] For these, transitions are observed between two levels for which the splitting, Δ, at zero field is smaller than the microwave quantum ($\sim$0.3 cm^{-1} at X-band). For $\Delta \approx h\nu$, these transitions are observed at very low fields. The shape of the signals is very sensitive to small variations in Δ. Within the previously introduced exchange-coupling model, we suggest that for isomer II the exchange interaction is large enough, so that the system behaves as an integer spin system. The theoretical spectra shown in Figure 2 are calculated for $J_1 = 0.99$ cm^{-1}, $J_2 = 0.63$ cm^{-1}, and $J_3 = 0.01$ cm^{-1} with the same $\mathbf{g_E}$ tensor as for Er@C_{82}(I). A distribution in J_i of 0.02 cm^{-1} was used, accounting for 3.6% of the isotropic value, $J = 0.543$ cm^{-1}. The larger exchange coupling in isomer II could indicate (other factors being equal) a somewhat smaller distance between Er^{3+} and the spin on the cage. Slight heterogeneities in this distance could explain the small distributions in the J values.

Our analysis suggests a large anisotropy for the **g**-tensor ($g_1 = 19$, $g_{2,3} < 1$) of the Er^{3+} ion in isomer I and probably in isomer II. This indicates that the crystal field symmetry around the Er^{3+} ion is low in analogy with Sc^{3+} in Sc@C_{82} for which the crystal structure has been determined by synchrotron X-ray powder diffraction.[11]

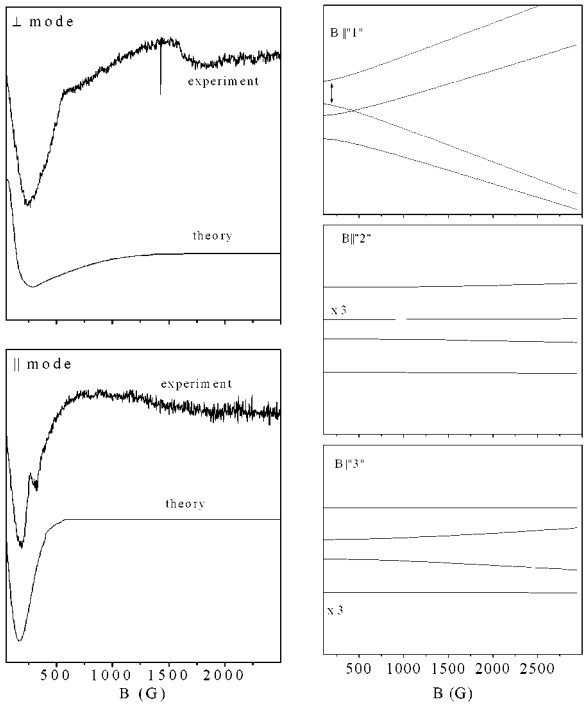

Figure 2. (Left panel) X-band EPR spectra of Er@C_{82}(II) for perpendicular and parallel polarization of the microwave field. The theoretical spectra were calculated as described in the text. The EPR conditions were identical to those for isomer I. (Right panel) Dependence of the energy levels on **B** for **B** along the three principal axes (1, 2, 3) of the $\mathbf{g_E}$ tensor. The arrow indicates the transition responsible for the spectra.

To the best of our knowledge, this is the first dual-mode EPR study of an endohedral metallofullerene. Of interest is the comparison of the present results with those of an earlier high-field EPR study of Er@C_{82}.[12] For a proper discussion, one should consider that in the present work we have studied two *different monometallofullerenes in isomer-pure form*. In the former study, apart from a mixture of isomers, some dimetallofullerenes, Er_2@C_{82} were also present. This indicates that those spectra represented at least three different species. In the presence of strong magnetic fields the Zeeman term decouples the exchange coupling of the metal with the cage (this condition is fulfilled for isomer I), hence, the presence of a free radical signal at $g \approx 2.005$ in the high-frequency spectra. The less defined low-field spectral region may then comprise signals from Er^{3+} of isomer I and the spectrum of isomer II. The exchange term for the latter may be significant even at high fields.

As a conclusion, X-band EPR spectroscopy can be used to differentiate metallofullerene isomers and gain insights into the metal−cage interactions.

Acknowledgment. We thank Professor M. Hendrich, Carnegie Mellon University, for providing us with the EPR simulation program, JSPS for support under the Future Program for New Carbon Nanomaterials (H.S.), and the Postdoctoral Program for Foreign Researchers (N.T.), and NEDO for support under the Frontier Carbon Technology Program (K.P.).

JA016636N

(8) In eq 1, we ignore hyperfine interactions with the ^{167}Er ($I = 7/2$) nuclei (natural abundance 24.4%).

(9) Theoretical powder spectra were obtained by diagonalization of eq 1 and summation of the EPR transition probabilities over a uniform spherical distribution of the magnetic field vector, **B**. The line shape was obtained with a homogeneous spin-packet line width σ_B, and a Gaussian distribution in the parameters **J** and $\mathbf{g_E}$ of width σ_J and σ_g, respectively.

(10) Hendrich, M. P.; Debrunner, P. G. *Biophys. J.* **1989**, *56*, 489−506.

(11) Nishibori, E; Takata, M.; Sakata, M.; Inakuma, M.; Shinohara, H. *Chem. Phys. Lett.* **1998**, *298*, 79−84.

(12) Boonman, M. E. J.; van Loosdrecht, P. H. M.; Bethune, D. S.; Holleman, I.; Meijer, G. J. M.; van Bentum, P. J. M. *Physica B* **1995**, *211*, 323−326.